

A control method for steering individual particles inside liquid droplets actuated by electrowetting

Shawn Walker*^a and Benjamin Shapiro^b

Received 20th September 2005, Accepted 10th October 2005

First published as an Advance Article on the web 27th October 2005

DOI: 10.1039/b513373b

An algorithm is developed that allows steering of individual particles inside electrowetting systems by control of actuators already present in these systems. Particles are steered by creating time varying flow fields that carry the particles along their desired trajectories. Results are demonstrated using an experimentally validated model developed in ref. 1. We show that the current UCLA electro-wetting-on-dielectric (EWOD) system² contains enough control authority to steer a single particle along arbitrary trajectories and to steer two particles, at once, along simple paths. Particle steering is limited by contact angle saturation and by the small number of actuators that are available to actuate the flow in practical electrowetting systems.

Introduction

In this paper, we demonstrate the possibility of using the available electrodes in an electro-wetting-on-dielectric (EWOD) device to actuate a single droplet in such a way that the resulting fluid flow inside the drop will carry a particle around a figure 8 path or carry two particles along separating trajectories. Steering particles inside droplets introduces another level of functionality into electro-wetting systems. For example, cells can be precisely placed over local sensors or moved from one location to another at rates much faster than those created by diffusion (see Fig. 1). In addition, particles can be sorted inside a droplet and then separated by controlled splitting of the droplet.

Our steering results are demonstrated using an experimentally validated numerical model¹ of droplet motion inside

the UCLA electrowetting system.^{2,3} This model of EWOD fluid dynamics includes surface tension and electrowetting interface forces, viscous low Reynolds 2-phase fluid flow, and the essential loss mechanisms due to contact angle saturation, triple point line pinning, and the related mechanism of contact angle hysteresis. To experimentally demonstrate particle steering in the UCLA EWOD device would require integration of a real-time implementation of our least squares based control algorithm with a real-time vision system to find the locations of particles and track droplet shapes. In this paper, we only show simulations that assume the visual feedback and ignore the real-time implementation issues.

Steering control algorithm

The electrode voltages in an EWOD device directly influence the pressure gradient field inside a droplet which, in turn, controls the velocity field.^{1,10,11} This allows us to steer multiple particles inside droplets by manipulating the fluid flow field through the voltages. Therefore, the control problem is to find an electrode voltage sequence that creates a temporally and spatially varying flow field that will carry all the particles along their desired trajectories.

^aAerospace Engineering, Research Assistant, University of Maryland at College Park, MD 20852, USA. E-mail: swalker@wam.umd.edu; Tel: +1 (301) 405-1998

^bAerospace Engineering, Joint appointment with Bio-Engineering graduate program and Institute of Systems Research, University of Maryland at College Park, MD 20852, USA. E-mail: benshap@eng.umd.edu; Tel: +1 (301) 405-4191

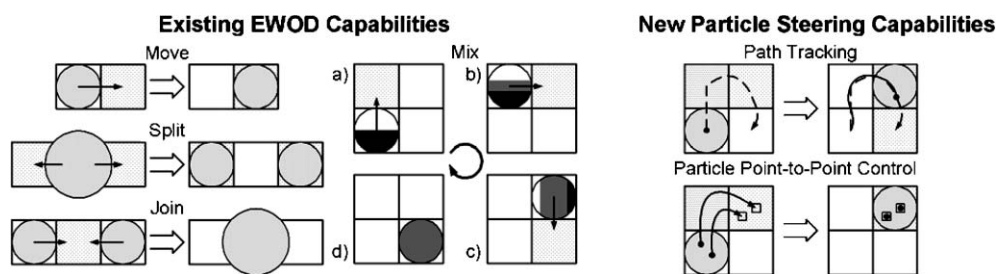


Fig. 1 The EWOD system manipulates fluids by charging a dielectric layer underneath the liquid that effectively changes the local surface tension properties of the liquid/gas interface creating liquid motion. Existing (move, split, join, and mix) capabilities of electrowetting devices are shown schematically above (see ref. 3, 4, 5, 6, 7, 8 and 9) alongside the new particle steering capability developed in this paper. The view is from the top of the EWOD device. Shaded circles represent droplets of liquid. Squares are electrodes where the dotted hatching indicates the electrode is on. Directed lines specify the direction of motion. The multi-shaded droplet shows the diffusion and mixing of two chemicals, here mixing is enhanced by the fluid dynamics created inside the droplet due to its imposed motion.

However, the particle motion depends on the droplet shape and the number of electrodes that the droplet overlays at any given moment. Since this is not known *a priori*, we use local estimation and control at each time step of our simulation to compute the pressure boundary conditions needed to realize the desired flow field. At each instant in time, the control algorithm is provided with the droplet shape and particle locations, as would be available through a vision sensing system. Any deviation of the particles from their desired trajectories that may arise from thermal fluctuations, external disturbances, and actuation errors is corrected using feedback of the particle positions. We now give an overview of our algorithm.

(1) *Initialization*: Represent the desired trajectory of each particle as a set of points connected by straight line segments.

(2) *Sensing*: Feedback the particle position data and the location of the droplet boundary to the control algorithm (as would be provided by the vision sensing system).

(3) *Control algorithm part A*: Choose the desired velocity directions of each particle so that the particles will move towards and then along the desired trajectories.

(4) *Control algorithm part B*: Solve a least squares problem for the necessary voltage actuations to induce a pressure gradient field that will create a flow field that will carry the particles along the desired directions obtained in step 3.

(5) *Actuate*: Apply the computed control voltages at the current time step of our simulation and advance the simulation to the next time step. This updates the droplet shape and particle positions. Then go back to step 2 and repeat the feedback control loop.

Step 4 of the algorithm requires more elaboration. Since the pressure field obeys Laplace's equation, which is linear, we can consider linear combinations of pressure boundary conditions due to voltage actuation at the electrodes (see Fig. 2). Hence, the problem of computing the necessary boundary conditions to create a pressure gradient field to move the particles in the directions we want, leads to a least squares problem which is given by the following.

First, knowing the current droplet configuration, we solve Laplace's equation for the pressure field inside the droplet due to a single active electrode. The pressure boundary conditions are defined to be one on the droplet boundary that lies over the active electrode and zero everywhere else (see Fig. 2). From the pressure solution, the pressure gradient at each particle's position is computed. After repeating this for each electrode, we obtain a matrix of pressure gradients

$$G = - \begin{bmatrix} \nabla P_1(x_1, y_1) & \cdots & \nabla P_N(x_1, y_1) \\ \vdots & \ddots & \vdots \\ \nabla P_1(x_m, y_m) & \cdots & \nabla P_N(x_m, y_m) \end{bmatrix} \quad (1)$$

where (x_j, y_j) are the coordinates for the j th particle. Each column of pressure gradients $\nabla P_k(x_j, y_j)$ in the matrix corresponds to a single active electrode; each row to a single particle. The total number of particles is m and the number of available electrodes is N . The minus sign accounts for the direction of particle motion. (In the example of Fig. 2 the droplet overlays 4 electrodes and there is one particle, so $N = 4$ and $m = 1$.)

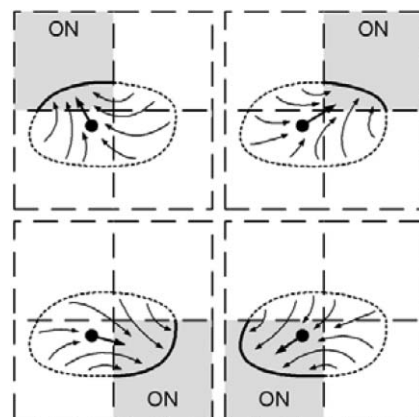


Fig. 2 Linear combination of pressure gradients for a single droplet overlaying four electrodes (small dashed squares). The diagram above shows a droplet in an EWOD system with four different instances of voltage actuation. In each instance, only one of the four electrodes is on. The particle floating inside the droplet (black dot) has a thick arrow indicating its direction of motion for each single electrode actuation. These arrows actually represent the opposite direction of the pressure gradient when a unit pressure boundary condition is set on the thick curve that overlays the shaded electrode, with zero pressure boundary conditions everywhere else. The thin curvy arrows show the fluid flow inside the droplet. Since the pressure field obeys Laplace's equation, it is linear and we can make the particle move in any desired direction by taking an appropriate linear combination of the four possible boundary conditions given above.

Next, we set the desired pressure gradient at particle j , $\nabla P_D(x_j, y_j)$, equal to the desired velocity direction (denoted b) obtained in step 3 of our algorithm. This gives the following linear system

$$G\alpha = b, \quad \alpha = \begin{bmatrix} \alpha_1 \\ \vdots \\ \alpha_N \end{bmatrix}, \quad b = \begin{bmatrix} \nabla P_D(x_1, y_1) \\ \vdots \\ \nabla P_D(x_m, y_m) \end{bmatrix} \quad (2)$$

where α is the vector of pressure boundary values that will achieve b . If $2m \geq N$, the number of particle degrees of freedom is greater than the available actuators and (in general) (2) cannot be solved exactly. A least squares solution is needed to obtain the best fit of actuations α . Otherwise, it is a pseudo-inverse problem, which has a solution as long as the matrix G has full row rank.¹²

We solve eqn (2) for α using the singular value decomposition (SVD).¹² However, the range of boundary pressure actuations is limited by contact angle saturation.^{13–16} Using experimental data on the saturation characteristics for the UCLA EWOD device,² we linearly map each component of the solution vector α so that these constraints are satisfied. As far as the steering algorithm is concerned, this mapping effectively changes the magnitude of b , which only affects the speed, and not the direction, of the particle motions. Hence, we choose the mapping so that the full dynamic range of boundary actuation is utilized, therefore maximizing the speed of the particles.

Finally, given that pressure on the boundary is directly related to the local contact angle,¹ we again use experimental data for the contact angle *versus* voltage characteristics of the

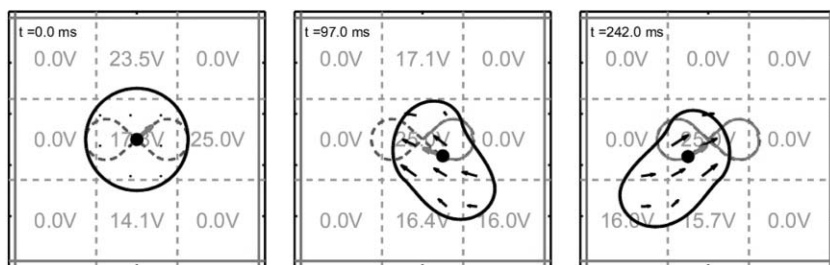


Fig. 3 Particle following a figure ‘8’ path. In the simulation results above, we have a droplet (denoted by the thick black curve) lying on a 3×3 grid of electrodes (denoted by the dashed lines). The dashed curve is the desired figure ‘8’ path and a black dot represents the particle with a thick grey arrow pointing in the desired direction of travel. The grey curve is the actual path of the particle. The black arrows inside the droplet denote the fluid velocity field inside the droplet. The voltages on the grid are time varying in such a way as to keep the particle moving along the desired path with less than 20 μm deviation.

EWOD device² to compute the electrode voltages needed to achieve the boundary pressures α . In general, there will be some uncertainty about the device parameters. In this paper, we do not consider adaptive or robust control strategies to deal with uncertain device parameters, but rather demonstrate the potential for particle control and separation in EWOD devices.

Results and discussion

Simulations were run assuming the device characteristics described in ref. 2. A 3×3 electrode grid was used to actuate and control the droplet where each square electrode is 1.4 mm on a side. All voltage actuations in these simulations are within the limits of the UCLA EWOD device.

In Fig. 3, a droplet is shown moving in a way that makes a particle floating inside follow a figure ‘8’ path. The droplet starts as a circle on the center electrode with a particle resting in its center. The voltages on the electrode grid are actuated using our

algorithm and, throughout the motion, the droplet always overlaps enough electrodes to allow it to be controlled in a way that keeps the particle moving forward on the desired trajectory.

In Fig. 4, we demonstrate particle separation. A droplet starts in the first panel with two particles spaced 0.31 mm apart. Both particles follow separate diverging trajectories designed to stretch the droplet and separate the particles. Once the particles near the ends of their trajectories (see the third frame), our control algorithm turns off and we command an open loop voltage of 25 V on the middle left and right electrodes and zero volts everywhere else. This causes the droplet to split into two smaller drops, each of which contains a single particle. The reason for not using our control algorithm to complete the split is because of numerical instability. When both particles are in the lobes of the dumbbell shape of the pinching droplet, the available forcing at the particles’ positions is fairly weak. This causes the condition number of the G matrix in eqn (2) to degenerate and produce errors in the least

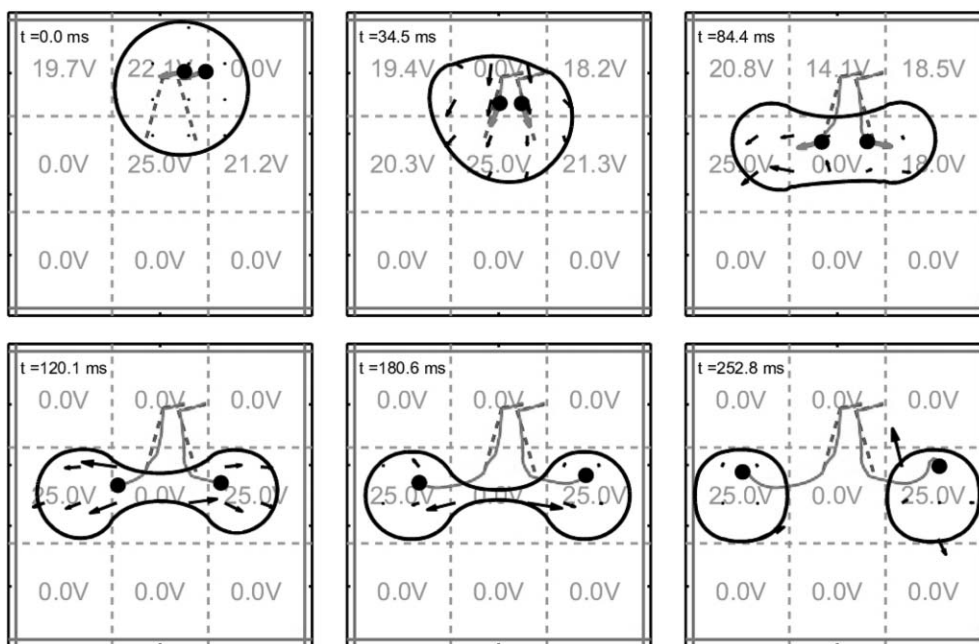


Fig. 4 Two-particle separation into two satellite drops (same format as in Fig. 3). Each particle first follows a trajectory that takes them away from each other. When there is sufficient distance between the two particles, our control algorithm turns off and the separation is completed by applying open loop voltages that split the droplet.

squares solution. Therefore, we avoid this by commanding open loop voltages that will split the droplet.²

Our simulations demonstrate the potential for performing particle placement and separation in the current UCLA EWOD devices with a reasonable number of electrodes. As of today, it is only feasible to fabricate devices with a few actuators that can control one or two particles. One of the limitations of achievable particle control arises from having a small number of electrodes available for actuation.

More particles or more complicated trajectories can require the droplet to become extremely distorted and necessitate splitting it into several pieces. Since the droplet has a natural tendency to remain in a circular shape because of surface tension, it is essential to have a large dynamic range in the pressure boundary forcing to overcome this. Contact angle saturation limits the boundary forcing and the degree of droplet deformation, which can cause particles to drift away from their desired trajectories as we have seen in our other numerical experiments. In addition, if two particles are very close together, the condition number of the matrix G degenerates. This causes numerical instability in solving eqn (2), which can lead to spurious oscillations in the control voltages.

It is interesting that existing EWOD systems have enough control authority to steer a single particle along complex trajectories and to steer two particles along simple paths. By designing a vision feedback control algorithm that exploits electro-wetting fluid dynamics, we have shown that existing EWOD actuation may achieve particle steering capabilities.

References

- 1 S. Walker and B. Shapiro, Modeling the Fluid Dynamics of Electro-Wetting on Dielectric (EWOD), *J. Microelectromech. Syst.*, 2004, submitted.
- 2 S. K. Cho, H. Moon and C.-J. Kim, Creating, Transporting, Cutting, and Merging Liquid Droplets by Electrowetting-Based Actuation for Digital Microfluidic Circuits, *J. Microelectromech. Syst.*, 2003, **12**, 1, 70–80.
- 3 J. Lee *et al.*, Electrowetting and electrowetting-on-dielectric for microscale liquid handling, *Sens. Actuators, A*, 2002, **95**, 269.
- 4 C. J. Kim, Micropumping by Electrowetting, in *International Mechanical Engineering Congress and Exposition*, New York, NY, IMECE2001/HTD-24200, 2001.
- 5 P. Paik, V. K. Pamula and R. B. Fair, A digital microfluidic biosensor for multianalyte detection, in *Proc. IEEE 16th Annual International Conference on Micro Electro Mechanical Systems*, Kyoto, Japan, 2003.
- 6 P. Paik, V. K. Pamula and R. B. Fair, Rapid droplet mixers for digital microfluidic systems, *Lab Chip*, 2003, **3**, 253–259.
- 7 M. G. Pollack, R. B. Fair and A. D. Shenderov, Electrowetting-based actuation of liquid droplets for microfluidic applications, *Appl. Phys. Lett.*, 2000, **77**, 11.
- 8 S. K. Cho, H. Moon, J. Fowler, S.-K. Fan, C.-J. Kim, Splitting a Liquid Droplet for Electrowetting-Based Microfluidics, in *International Mechanical Engineering Congress and Exposition*, New York, NY, IMECE2001/MEMS-23831, 2001.
- 9 J. Fowler, H. Moon and C.-J. Kim, Enhancement of Mixing by Droplet-Based Microfluidics, *IEEE Conf. MEMS, Las Vegas, NV*, 2002, pp. 97–100.
- 10 R. L. Panton, *Incompressible Flow*, 2nd edn, 1996, New York, NY, John Wiley & Sons, Inc.
- 11 G. K. Batchelor, *An Introduction to Fluid Dynamics*, 1967, Cambridge University Press.
- 12 G. Strang, *Linear Algebra and Its Applications*, 3rd edn, 1988, New York, NY, Brooks Cole.
- 13 B. Shapiro, Equilibrium Behavior of Sessile Drops under Surface Tension, Applied External Fields, and Material Variations, *J. Appl. Phys.*, 2003, **93**, 9.
- 14 M. Vallet, M. Vallade and B. Berge, Limiting phenomena for the spreading of water on polymer films by electrowetting, *Eur. Phys. J.*, 1999, **11**, B, 583–591.
- 15 H. J. J. Verheijen and W. J. Prins, Reversible electrowetting and trapping of charge: Model and experiments, *Langmuir*, 1999, **15**, 6616–6620.
- 16 F. Mugele and J.-C. Baret, Electrowetting: from basics to applications, *J. Phys.: Condens. Matter*, 2005, **17**, 28, 705–744.